Article

Physicochemical and Computational Study of the Encapsulation of Resv-4′-LA and Resv-4′-DHA Lipophenols by Natural and HP-β-CDs

Ana Belén Hernández-Heredia , Dennis Alexander Silva-Cullishpuma , José P. Cerón-Carrasco , Angel Gil-Izquierdo , Jordan Lehoux , Léo Faion , Céline Crauste , Thierry Durand , José Antonio Gabaldón * , Estrella Núñez-Delicado *

Posted Date: 8 July 2025

doi: 10.20944/preprints202507.0673.v1

Keywords: Lipophenols; fatty acids; cyclodextrins; bioactive compounds; micelles; nanoencapsulation

 doi:10.20944/preprints202507.0673.v1

Article

Physicochemical and Computational Study of the Encapsulation of Resv-4′-LA and Resv-4′-DHA Lipophenols by Natural and HP-β-CDs

Ana Belén Hernández-Heredia [1], Dennis Alexander Silva-Cullishpuma [1], José Pedro Cerón-Carrasco [2], Ángel Gil-Izquierdo [3], Jordan Lehoux [4], Léo Faion [4], Céline Crauste [4], Thierry Durand [4], José Antonio Gabaldón [1,*] and Estrella Núñez-Delicado [1,*]

[1] Molecular Recognition and Encapsulation Research Group (REM), Health Sciences Department, Universidad Católica de Murcia (UCAM), Campus de los Jerónimos 135, E-30107 Guadalupe, Spain

[2] Centro Universitario de la Defensa, Universidad Politécnica de Cartagena, C/Coronel López Peña s/n, Base Aérea de San Javier, E-30720 Santiago de la Ribera, Spain

[3] Research Group on Quality, Safety, and Bioactivity of Plant-Derived Foods, Department of Food Science and Technology, CEBAS-CSIC, Campus de Espinardo-25, E-30100 Murcia, Spain

[4] Institut des Biomolécules Max Mousseron (IBMM), Pôle Chimie Balard Recherche, UMR 5247-CNRS, Faculty of Pharmacy, Université de Montpellier-ENSCM, Montpellier, France

* Correspondence: jagabaldon@ucam.edu (J.A.G.); enunez@ucam.edu (E.N.-D.); Tel.: +34-968-278869

Abstract

This study investigates the self-assembly and host-guest complexation behaviour of novel resveratrol-based lipophenols (LipoResv) – resveratrol-4′-linoleate (Resv-4′-LA) and resveratrol-4′-docosahexaenoate (Resv-4′-DHA) – with hydroxypropyl-β-cyclodextrins (HP-β-CDs). These amphiphilic molecules display surfactant-like properties, forming micellar aggregates in aqueous media. Fluorescence spectroscopy was used to determine the critical micelle concentration (CMC), revealing that LipoResv exhibit significantly lower CMC values than their free fatty acids, indicating higher hydrophobicity. The formation of inclusion complexes with HP-β-CDs was evaluated based on changes in CMC values and further confirmed by dynamic light scattering (DLS) and molecular modelling analyses. Resv-4′-LA formed 1:1 complexes (Kc= 720 M^{-1}), while Resv-4′-DHA demonstrated 1:2 stoichiometry with lower affinity constants (K_1= 17 M^{-1}, K_2= 0.18 M^{-1}). Environmental parameters (pH, temperature and ionic strength) significantly modulated CMC and binding constants. Computational docking and molecular dynamics simulations supported the experimental findings by revealing key structural determinants of host-guest affinity and micelle stabilization. Ligand efficiency (LE) analysis further aligned with the experimental data, favouring the unmodified fatty acids. These results highlight the versatile encapsulation capacity of HP-β-CDs for bioactive amphiphiles molecules and support their potential applications in drug delivery and functional food systems.

Keywords: Lipophenols; fatty acids; cyclodextrins; bioactive compounds; micelles; nanoencapsulation

1. Introduction

Polyphenols and essential omega-3-polyunsaturated fatty acid (n-3 PUFA) have been widely recognized as molecules with premium beneficial effects for health [1,2]. On the other hand, chemical bonding between the two structures leading to n-3 lipophenol derivatives (or phenolipids) has been studied in a growing number of works over the last decade. Some examples of lipophenol-related studies highlighted their presence in food or vegetable matrices, while other have reported synthetic

 doi:10.20944/preprints202507.0673.v1

lipophenol developed for therapeutic application [3]. They have been designed to link in a same molecule, the potential health benefices of both, the polyphenol and the fatty acid, and at the same time increase the hydrophobicity of weak hydrophobic polyphenol for a better cell penetration, and protection of oxidation in lipid membrane or lipid rich tissue [4]. In this context, we have previously synthesised combinations of resveratrol with linoleic or docosahexaenoic acids, resveratrol-4'-linoleate (Resv-4'-LA) and resveratrol-4'-docosahexaenoate (Resv-4'-DHA), respectively, for testing their activity to reduce oxidative stress in retinal pigment epithelial cells for age-related macular degeneration purposes [5]. In addition, in *in vitro* assays (Resv-4'-LA) exhibited a drastic reduction of the exacerbated pathological endothelial permeability by inhibiting the activity and expression of MMP-9 metalloproteases and consequently, preserving the endothelial intercellular junction integrity [6], being a promising group contributing to the absence of pathological events in populations, that are already at risk and predisposed to occur (primary prevention) or improving the ischemic damage, with already established pathological events of relatively reduced or controlled extent (secondary prevention).

Despite the plausible potential effects of this compounds, his accentuated hydrophobic nature, the difficulty of obtaining it by chemical or enzymatic synthesis with good yields, the scarcity of work related to their mapping in plants, as well as *in vitro* and *in vivo* assays that shed some light on their bioavailability, absorption and metabolism, we recommend urgently addressing this task, attempting to solve low aqueous solubility by using cyclodextrins (CDs) for later preclinical assays.

The solubilization of bioactive compounds remains a significant challenge in food, pharmaceutical and biomedical research. In fact, resveratrol lipophenols or resveratrol phenolipids (LipoResv) are amphiphilic molecules composed of some polar head group (resveratrol), and a hydrophobic aliphatic chain derived from fatty acids (Figure 1). In aqueous environments, the hydrophobic segments tend to associate through hydrophobic interactions, resulting in the formation of a non-polar core that excludes water molecules. Concurrently, the polar head groups orient towards the surrounding aqueous phase.

This amphiphilic nature drives the spontaneous self-assembly of LipoResv into organized supramolecular structures, analogous to those formed by classical lipids [7].

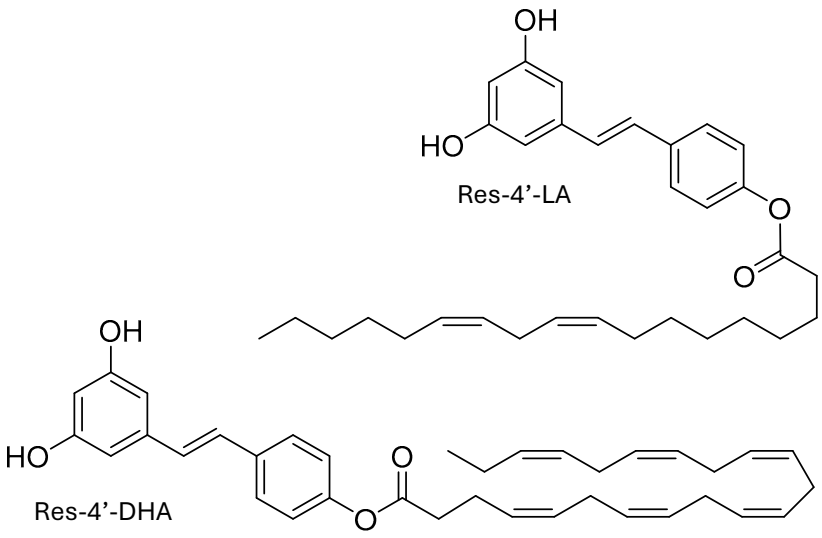

Figure 1. Structure of resveratrol lipophenols (LipoResv): resveratrol-4'-linoleate (Resv-4'-LA) and resveratrol-4'-docosahexaenoate (Resv-4'-DHA).

Micellar systems are commonly employed as supramolecular hosts to enhance the solubilization of different poorly water-soluble compounds [8]. The ability of lipophenols to self-assemble into micelle-like aggregates imparts dual functionality, enabling them to act both as host molecules and as structural components of micellar assemblies. This dual role introduces additional complexity to

 doi:10.20944/preprints202507.0673.v1

the equilibria in solution, as their behaviour is highly dependent on the surrounding environment [9].

Like micellar systems, cyclodextrins (CDs) have been widely used for the solubilization of poorly water-soluble drugs and other hydrophobic compounds [10,11]. CDs are cyclic oligosaccharides with a hydrophobic cavity, enabling the formation of dynamic inclusion complexes with hydrophobic molecules [12]. β-CDs are the most accessible and widely used native type, while numerous derivatives with modified properties have been synthesized. Inclusion in CDs alters the physicochemical properties of guest molecules, enhancing solubility, stability and controlled release, among other effects. This versatility makes CDs valuable in diverse fields, including food, pharmaceuticals, cosmetics, and environmental applications [10,13-15].

It is important to note that the complexation ability of CDs is influenced not only by the specific type of CDs employed, but also by the physicochemical characteristics of the guest molecule [11]. In this sense, the efficiency and stability of complex formation can vary depending on the compatibility between the structural and chemical properties of the host and guest [16]. Furthermore, multiple modes of inclusion are possible [10,17]. Unlike micellar systems, CDs are structurally well-defined and do not rely on aggregation equilibria for their functionality. Nevertheless, their inclusion capacity and interaction with guest molecules can be significantly modulated by external conditions such as temperature, pH and ionic strength [18].

The critical micelle concentration (CMC) is a fundamental characteristic of surfactants, representing the concentration at which self-assembly into micelles begins. Due to their amphiphilic nature, lipophenols exhibit surfactant-like behaviour [19]. The formation of micelles induces measurable changes in various physicochemical properties of the solution, providing each one an analytical signal that can be measured and transduced to obtain a parametric value applying a chemical measurement process. Consequently, several analytical techniques such as electrical conductivity, surface tension measurements, nuclear magnetic resonance (NMR) spectroscopy, UV-Vis absorption, or fluorescence spectroscopy, between others, can be employed to determine the CMC [12,18-22].

It is important to recognize that not all analytical methodologies are universally applicable to every compound; the selection of as appropriate technique must be guided by the specific physicochemical behaviour of the compound under study [23]. The wide range of empirical approaches available for determining the CMC likely reflects the inherent complexity of the micellization process. Although there are advanced models and simulations that describe micelle formation in detail, these are often not designed to analyse experimental data directly. As a result, they usually do not include equations where the CMC can be used as a fitting parameter.

The use of fluorometric method for determining the CMC is motivated, in part, by their higher sensitivity and accuracy, particularly for compounds with low CMC values [20]. This approach offers advantages over other techniques that may be less effective, due to technical limitations or incompatibility with the physicochemical properties of certain compounds [24].

This is the first study to analyse the complexation between CDs and LipoResv. In this work, we studied the structural and aggregation behaviour of LipoResv, specifically resveratrol-4′-linoleate (Resv-4′-LA) and resveratrol-4′-docosahexaenoate (Resv-4′-DHA), in the presence of CDs. Moreover, the effect of hydroxypropyl-β-cyclodextrins (HP-β-CDs) concentration, temperature, pH and ionic strength in the complexation process will be evaluated. To elucidate the aggregation behaviour of LipoResv and to investigate the mechanism of complexation with HP-β-CDs across different environmental conditions, fluorescence spectroscopy was employed to determine the CMC, while dynamic light scattering (DLS) was used to assess particle size and aggregation profiles. These experimental findings are further supported by computational models, providing insight into the molecular interactions underlying the complexation process.

2. Results and Discussion

 doi:10.20944/preprints202507.0673.v1

LipoResv (Resv-4′-LA and Resv-4′-DHA) behaved like fatty acids in aqueous solution, forming micellar aggregates due to their amphiphilic nature (Figure 1). Moreover, in the presence of CDs, inclusion complexes were formed above a concentration of fatty acid (Figure 2A,B) or LipoResv (Figure 2C,D), and an equilibrium was established between micellar aggregates, free and complexed LipoResv or fatty acid [25], as was previously described by Bru et al. for unsaturated fatty acids.

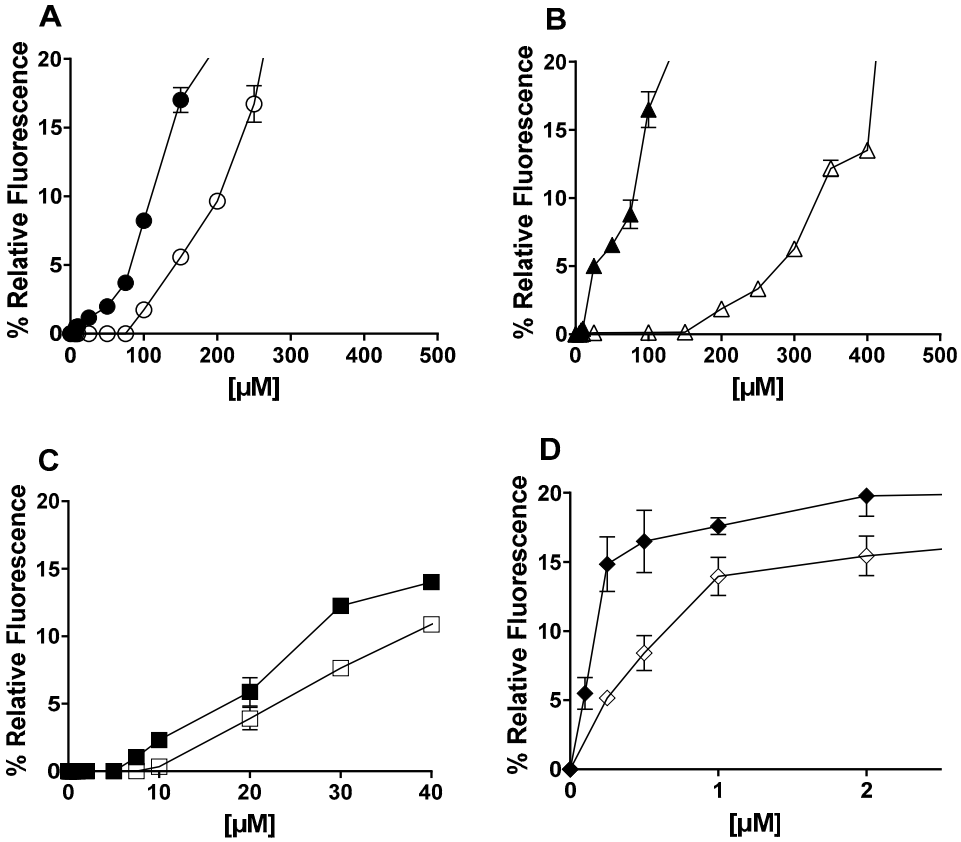

Figure 2. Relative fluorescence at 430 nm (excitation 358 nm) according to the concentration of (resveratrol-4′-linoleic acid (Resv-4′-LA), Resv-4′-DHA, linoleic acid (LA) and docosahexaenoic acid (DHA) in the absence and in the presence of hydroxypropyl-β-cyclodextrins (HP-β-CDs) in 100 mM sodium phosphate buffer (PBS) pH 7.0 and 35°C. (A) ● LA, ⊖ 0.25 mM HP-β-CDs/LA; (B) ▲ DHA, △ 0.25 mM HP-β-CDs/DHA; (C) ■ Resv-4′-LA, ⊟ 0.25 mM HP-β-CDs/ Resv-4′-LA; (D) ◆ Resv-4′-DHA, ◇ 0.25 mM HP-β-CDs/ Resv-4′-DHA.

The CMC calculation through the measurement of fluorescence by means of a probe such as DPHT [26], was the methodology used to study the behaviour of the aggregates at increasing concentrations of LipoResv and the formation of inclusion complexes with CDs, although there are other methodologies to determine the CMC that are also valid [18], such as DLS [27], conductivity, surface tension [20], etc.

2.1. LipoResv CMC

In aqueous solution, the point at which aggregates start to form is specific for each compound and the assay conditions. As can be seen in Figure 2, Resv-4′-LA and Resv-4′-DHA (Figure 2C,D), as well as their respective fatty acids, LA and DHA (Figure 2A,B), increased relative fluorescence, indicating the formation of aggregates above a certain critical concentration, this being the CMC.

The free fatty acids LA (Figure 2A) and DHA (Figure 2B) needed a higher concentration than their respective LipoResv (Figure 2C,D) to form micelles in aqueous solution, that is, the CMC_0 for LA or DHA, were higher than those obtained for Resv-4′-LA and Resv-4′-DHA. The CMC_0 at pH 7.0 for LA and Resv-4′-LA, were 43 and 6 μM, respectively, and in the case of DHA and Resv-4′-DHA they were 70 and 0.001 μM, respectively. These results, in which CMC_0 decreased 7 and 70,000-fold for Resv-4′-LA and Resv-4′-DHA, respectively, should be explained by the substitution of the polar

 doi:10.20944/preprints202507.0673.v1

head of the fatty acid with resveratrol molecule, resulting in a new significantly more hydrophobic compound.

Comparing Resv-4'-LA and Resv-4'-DHA, the CMC_0 of Resv-4'-LA was 6,000-fold higher than the CMC_0 of Resv-4'-DHA, indicating the much lower aqueous solubility of Resv-4'-DHA. The CMC_0 can be considered as a measure of the self-association tendency of each amphiphilic compound and depends on several parameters. In general, the more surface active the amphiphilic compound, the higher the tendency to micellization and, therefore, the lower its CMC_0. Therefore, the longer the total length of the hydrocarbon chain of a fatty acid, the lower the CMC [23,26,28].

As has been described in the literature [26] the incorporation of CDs to a fatty acid solution yield to an increase in the CMC value, due to the complexation of fatty acid in the internal cavity of the CDs. This CMC change depends on the capability of each specific type of CDs to complex each specific fatty acid. To study the effect of the addition of CDs to aqueous solutions of LipoResv, different types of β-CDs were analysed (β-CDs, HP-β-CDs and methyl-β-CDs) by computational simulations. The results obtained showed that HP-β-CDs were the most optimal for the LipoResv encapsulation (Table S1).

The incorporation of HP-β-CDs in the reaction medium yielded an increase of CMC_0 in all cases, indicating an increased in the aqueous solubility for both, free fatty acids (Figure 2A,B) and LipoResv (Figure 2C,D), the increase being more pronounced in the case of free fatty acids (Figure 2A,B). The addition of 0.25 mM of HP-β-CDs increased the CMC of LA from 43 to 136 μM (3.2-fold) and in the case of DHA from 70 to 185 μM (2.6-fold). However, in the case of LipoResv the increase in CMC were lower, from 6 to 8.8 μM (1.5-fold) in the case of Resv-4'-LA and from 0.001 to 0.002 μM (2-fold) in the case of Resv-4'-DHA.

These increases in CMC_0 values were due to the complexation process of fatty acids and their respective LipoResv in the hydrophobic cavity of HP-β-CDs, as described previously Matencio et al. for conjugated LA [29]. The complexation process is directly related to the solubility of the compound. An increase in the hydrophobicity of a compound leads to an increase in its affinity to complex in the hydrophobic cavity of CDs but simultaneously implies an increase in its tendency to form micelles [22,28].

Figure 3 shows a detailed representation in which the relative fluorescence increased with the HP-β-CDs concentration in the reaction medium, clearly indicating a delay in the micelle formation by Resv-4'-LA and thus, in the CMC due to the complexation of Resv-4'-LA in the hydrophobic cavity of CDs. These results align with those reported by other research groups on fatty acids, confirming their dual behaviour in the presence of CDs as a function of concentration [26].

Although the CMC is often reported as a single numerical value, it is not a sharply defined quantity. In practice, micellization occurs over a concentration range, and the value obtained can vary depending on the experimental method employed [18], leading to challenges in its accurate determination [22]. Furthermore, as previously observed, the molecular structure of the amphiphilic compounds is not the sole determinant of the CMC. Owing to the entropically driven nature of micelle formation, the CMC is also influenced by several environmental factors [7, 17] including ionic strength, pH and temperature as will be further discussed below.

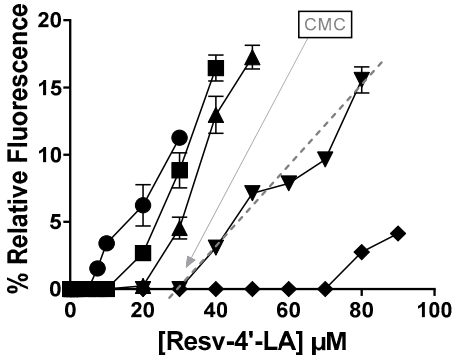

 doi:10.20944/preprints202507.0673.v1

Figure 3. Influence of HP-β-CDs concentration in the relative fluorescence for Resv-4′-LA at pH 7.0 and 35 °C: ● 0 mM HP-β-CDs; ■ 1 mM HP-β-CDs; ▲ 2 mM HP-β-CDs; ▼ 5 mM HP-β-CDs; ◆ 10 mM HP-β-CDs.

2.2. Stoichiometry and Kc of the Complexes LipoResv and CDs

By studying the CMC behaviour of Resv-4′-LA and Resv-4′-DHA with increasing concentrations of HP-β-CDs, the stoichiometry and the Kc value for the complexation processes were determined. As can be seen in Figure 4, the CMC increased with HP-β-CDs concentration in all cases, LA (Figure 4A), Resv-4′-LA (Figure 4B), DHA (Figure 4C) and Resv-4′-DHA (Figure 4D), indicating that the complexation of fatty acids and LipoResv in the hydrophobic cavity of CDs delayed micelles formation.

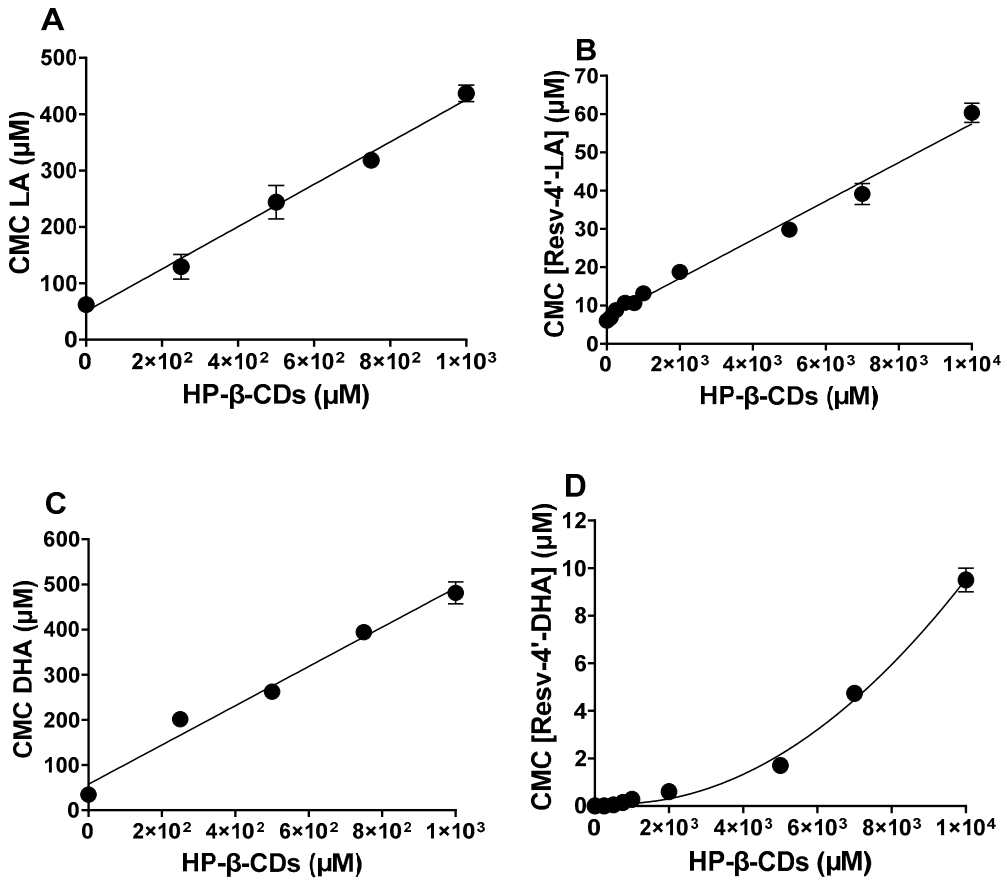

Figure 4. Effect of HP-β-CDs concentration in the critical micellar concentration (CMC) value of LipoResv and its fatty acids at 35 °C and pH 7.0. (A) LA (B) Resv-4′-LA (C) DHA (D) Resv-4′-DHA.

In the case of Resv-4′-LA, a linear dependence of the CMC with HP-β-CDs concentration was observed (Figure 4B), as in the case of LA (Figure 4A), indicating a 1:1 stoichiometry for complexation process in both cases. The Kc value for Resv-4′-LA was calculated by linear regression to the Equation 1 and the value obtained was 720 M^{-1} at pH 7.0 and 35 °C. Comparing the results obtained for Resv-4′-LA (Figure 4B) and its fatty acid counterpart (LA) (Figure 4A), revealed also a 1:1 stoichiometry consistent with results reported previously by other authors [25]. When Kc between LA and HP-β-CDs was calculated, a value of 7,432 $M^{-1}$was obtained. This value was 10-fold higher than that obtained between Resv-4′-LA and HP-β-CDs, indicating that the complexation between LA and HP-β-CDs is much more stable than between Resv-4′-LA and HP-β-CDs at the same conditions.

Although the most frequent stoichiometry described in the literature for the complexation with HP-β-CDs is 1:1, some molecules may also form 1:2 complexes [17,30].

When the complexation process of Resv-4′-DHA was analysed, it could be observed that the CMC also increased with HP-β-CDs concentration, but clearly in a non-linear way (Figure 4C),

 doi:10.20944/preprints202507.0673.v1

indicating a probably 1:2 stoichiometry for the complexes formed. That is, each molecule of Resv-4'-DHA could be complexed by two molecules of HP-β-CDs. This coupling process could occur simultaneously, with a single Kc value, or sequentially with two complexation constants ($K_{1:1}$ and $K_{1:2}$) (Scheme 1).

$$[CDs] + [LipoResv] + [CDs] \xrightarrow{Kc} [2CDs/LipoResv] \quad \text{(simultaneous)}$$

$$[CDs] + [LipoResv] \xrightarrow{Kc_1} [CDs/LipoResv] + [CDs] \xrightarrow{Kc_2} [2CDs/LipoResv] \quad \text{(sequentially)}$$

Scheme 1

Scheme 1.

Fitting the data presented in Figure 4D to Equation 4, the results indicated that the coupling process between Resv-4'-DHA and HP-β-CDs occurs sequentially, resulting in two equilibrium constants: $K_1 = 17\ M^{-1}$ and $K_2 = 0.18\ M^{-1}$. The fact that the value of K_2 was lower than that for K_1, could be due to the complexation process was produced stepwise binding energetic where the coupling of the first HP-β-CDs had a moderate stability, and the second one binding energy was reduced due to the most hydrophobic regions of the Resv-4'-DHA were already shielded by the first HP-β-CDs, leaving weaker interactions for the second HP-β-CDs. Although relatively low, it is not uncommon for K_2 to be smaller than K_1. The formation of the 1:2 complexes proceed through an initial 1:1 complex formation, which can restrict the spatial orientation and available surface area for the binding of the second CDs molecule.

Triamchaisi et al. in 2023 observed that both 1:1 and 2:1 stoichiometries of β-CDs with cannabidiol and tetrahydrocannabinol were feasible. The 2:1 complex exhibited more favourable complexation energies and greater chemical stability compared to the 1:1 complex. However, the Kc for the 2:1 complex was lower than that observed for the 1:1 complex [31].

In case of DHA, a linear dependence between CMC and HP-β-CDs was observed, indicating a 1:1 stoichiometry between DHA and HP-β-CDs (Figure 4C), in contrast to the nonlinear dependence observed for Resv-4'-DHA. Fitting the experimental data with linear regression the Kc value obtained was $7{,}557\ M^{-1}$. This value was like that obtained for LA and HP-β-CDs, indicating that this type of modified CDs form complexes with similar stability in both cases, LA and DHA, probably due to their similar aqueous solubility (CMC of LA 50.5 µM and CMC of DHA 57.5 µM).

While it is evident that increasing CDs concentration elevated the CMC, determining Kc proves challenging due to different factors: the significant variability in CMC values arising from the equilibrium between CDs and LipoResv describing CDs complexes with 1:1 and 1:2 stoichiometry [32]; the presence of various conformations [33,34]; the formation of aggregates with different sizes as a result of CDs incorporation [35] and the difficulty in establishing a stable S_0 in highly insoluble compounds [14].

Although the literature commonly reports that CDs exhibit greater affinity toward more hydrophobic compounds [10], this trend has not been observed in the present study. This discrepancy highlights the importance of evaluating each compound individually, as CDs–guest interactions could be influenced by factors beyond hydrophobicity, such as molecular size, geometry and the distribution of functional groups of guest molecule. Furthermore, it should be considered that the determination of the CMC is inherently complex, particularly in systems containing CDs. As demonstrated Yun-Bao Jiang and Xiu-Juan Wang, the formation of CDs inclusion complexes can significantly alter the aggregation behaviour of surfactants. Specifically, the 1:1 β-CDs/surfactant complex may act as an alternative hydrophobic core, promoting surfactant monomer aggregation even at concentrations below the conventional CMC [36].

 doi:10.20944/preprints202507.0673.v1

2.3. Particle Size in Relation to CMC and Complexes Formation

DLS was employed to estimate the hydrodynamic diameter of the micelles and to assess the PDI of the system at 35 °C and pH 7.0 for both Resv-4′-LA and Resv-4′-DHA (Figure 5).

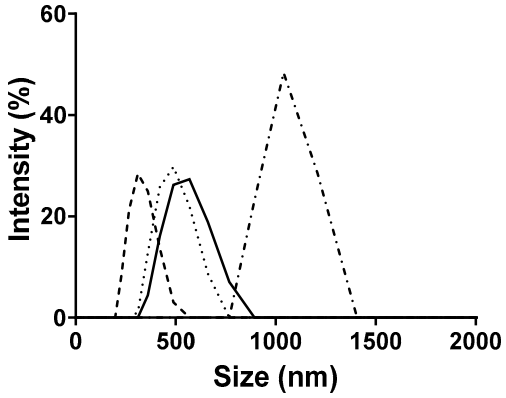

Figure 5. Particle size (nm) by dynamic light scattering (DLS): Resv-4′-LA 10 μM (- - -), Resv-4′-LA 50 μM (—), Resv-4′-DHA 10 μM (· · · ·) and Resv-4′-DHA 50 μM (- · -) in PBS at 35 °C and pH 7.0.

The average micelle size and the PDI were found to vary as a function of LipoResv and HP-β-CDs concentration, indicating a heterogeneous population of particle size.

The results presented in Figure 5 demonstrated that the particle size increased with the LipoResv concentration. At a fixed concentration of 10 μM of LipoResv, the particle size for Resv-4′-LA and Resv-4′-DHA were 438 (Figure 5, - - -) and 600 nm (Figure 5, · · · ·), respectively. However, when the LipoResv concentration increased to 50 μM, the particle size for Resv-4′-LA increased to 622 nm (Figure 5, —), (1.4-fold), and for Resv-4′-DHA increased to 2989 nm (Figure 5, - · -), (5-fold). These findings suggested that Resv-4′-LA exhibited greater aqueous solubility compared to Resv-4′-DHA. This interpretation aligns with the CMC_0 values obtained in the absence of CDs, which were 6 μM for Resv-4′-LA (Figure 2C) and 0.001 μM for Resv-4′-DHA (Figure 2D). The lower CMC_0 of Resv-4′-DHA (6,000-fold) indicated that micelle formation occurred at much lower concentration that in the case of Resv-4′-LA, due to the lower aqueous solubility of Resv-4′-DHA (Table 1).

The presence of HP-β-CDs may lead to their inclusion within the micellar system, thereby increasing the overall size [35,37]. It is also possible that CDs complexes self-assemble into larger aggregates, as previously reported in the literature [36]. Although an increase in particle size was observed in our experimental system, the incorporation of HP-β-CDs may contribute to reduction in micellar aggregation by encapsulating LipoResv [37].

Table 1. CMC, complexation constant (Kc), particle size (nm) and polydispersity index (PDI) of Resv-4′-LA and Resv-4′-DHA in the presence of HP-β-CDs.

LipoResv	Concentration (μM)	HP-β-CDs (mM)	Size (nm)	PDI	CMC (μM)	K_C (M^{-1})
Resv-4′-LA	10	0	438	0.42	6	719
		10	89	0.57		
	50	0	622	0.21		
		10	894	0.37		
Resv-4′-DHA	10	0	600	0.31	0.001	K_1: 17; K_2: 0.18
		10	943	0.46		
	50	0	2,989	0.73		
		10	3,835	0.95		

To evaluate the colloidal stability of the particles analysed by DLS, 50 μM Resv-4′-LA solutions were prepared in the presence and absence of HP-β-CDs, initially characterized, and then stored at

 doi:10.20944/preprints202507.0673.v1

room temperature in the dark for 24 hours before a second DLS measurement was performed. Subsequent particle size measurements revealed an increase. Initially, the particle size of Resv-4'-LA in the absence of HP-β-CDs was 622 nm, increasing to 933 nm after 24 hours (1.5-fold). Moreover, in the presence of HP-β-CDs, the initial particle size was 894 nm, which increased to 1,073 nm (1.2-fold) after 24 hours of storage.

2.4. Influence of pH, Temperature and Ionic Strength on LipoResv CMC and Complexation Process

As micellization tendency of amphiphilic molecules and complexation in CDs processes could be affected by temperature, pH and ionic strength, the effect of these parameters for Resv-4'-LA and Resv-4'-DHA in the presence of HP-β-CDs were studied. Although changes in temperature (15, 25 and 35 °C), pH (2.0 and 7.0) and salt concentration (PBS 100 mM and MilliQ water) did not cause changes in the CMC's profile with the concentration of HP-β-CDs, linear in the case of Res-4'-LA and nonlinear in the case of Res-4'-DHA, produced variations in CMC and equilibrium constants values for both Res-4'-LA and Res-4'-DHA (Table 2).

Table 2. CMC and Kc of Resv-4'-LA and Resv-4'-DHA at different temperatures (35, 25 and 15 °C), pHs (7,0 and 2,0) and ionic strength (PBS 100 mM and MilliQ water).

LipoResv	Temperature (ºC)	pH	Medium	CMC (μM)	Kc (M^{-1})
Resv-4'-LA	35	7.0	PBS	6.00	720
	25	7.0	PBS	0.27	8,157
	15	7.0	PBS	0.14	10,432
	35	2.0	PBS	0.54	4,347
	35	7.0	MilliQ	0.11	42,535
Resv-4'-DHA	35	7.0	PBS	$1x10^{-3}$	K_1: 17; K_2: 0.18
	25	7.0	PBS	$6x10^{-4}$	K_1: 787; K_2: 0.10
	15	7.0	PBS	$3x10^{-4}$	K_1: 898; K_2: 0.33
	35	2.0	PBS	$5x10^{-4}$	K_1: 97; K_2: 0.45
	35	7.0	MilliQ	$5x10^{-4}$	K_1: 707; K_2: 0.33

As can be seen in Table 2, the acidification of the pH of the reaction medium (pH 7.0 to pH 2.0) involved a decrease in CMC_0 in both cases. For Resv-4'-LA, the CMC_0 decreased form 6 μM at pH 7.0 to 0.54 μM at pH 2.0, and from 0.001 to $5x10^{-4}$ μM in the case of Resv-4'-DHA, indicating a lower solubility of LipoResv at acidic pH in both cases, but with a more pronounced decrease in the case of Resv-4'-LA. Moreover, a decrease in the temperature also affected to the CMC_0 values, diminishing from 6 μM at 35 °C to 0.27 μM at 25 °C and 0.14 μM at 15 ºC in the case of Resv-4'-LA; and from 0.001 to $6x10^{-4}$ and $3x10^{-4}$ μM, respectively in the case of Resv-4'-DHA. The ionic strength of the reaction medium interfered in micelle formation, decreasing CMC_0 of Resv-4'-LA from 6 to 0.11 μM and in the case of Resv-4'-DHA from 0.001 to $5x10^{-4}$ μM, when the reaction medium was MilliQ water.

The decrease observed in CMC_0 with pH, temperature and ionic strength also implied changes in the Kc values for both LipoResv in the presence of HP-β-CDs. For Resv-4'-LA, a decrease in the pH leaded to an increase in Kc value from 720 to 4,264 M^{-1}. In the case of Resv-4'-DHA, where 1:2 complexes were formed, the K_1 value increased from 17 to 97 M^{-1}, and K_2 from 0,18 to 0,45 M^{-1} (Table 2). When temperature decreased from 35 to 25 and 15 °C, the Kc values increased from 720 to 8,157 and 10,432 M^{-1}, respectively, for Resv-4'-LA and from 17 and 0.18 M^{-1} for K_1 and K_2, respectively, to 787 and 0.1 M^{-1} at 25 °C; and to 898 and 0.33 M^{-1} at 15 ºC in the case of Resv-4'-DHA. In the absence of salt in the reaction medium, Kc values increased for LipoResv. In the case of Resv-4'-LA, Kc value increased from 719 to 42,535 M^{-1} and from 17 to 707 M^{-1} in the K_1 value and from 0.18 to 0.33 M^{-1} in the K_2 one in the case of Resv-4'-DHA (Table 2).

These results obtained with the pH changes could be explained by the stabilization of the hydrocarbon chain of the fatty acid in an acidic media. By lowering the pH, the carboxyl group of the fatty acid and the -OH group of the HP-β-CDs remain intact and favour the formation of hydrogen

 doi:10.20944/preprints202507.0673.v1

bonds between LipoResv and the hydrophobic cavity of the HP-β-CDs. Moreover, the non-deprotonated form of the LipoResv is more hydrophobic, thus favouring its entry into the internal cavity of the HP-β-CDs through hydrophobic interactions. When a molecule is in its neutral form, exhibits increased hydrophobic character respect to its ionic form, which reduces electrostatic interactions with CDs providing a better fit within their hydrophobic cavity [38,39]. Furthermore, an increase in temperature leads to a rise in molar conductivity, which is attributed to a reduction in viscosity and an enhanced in ions mobility within the solvent, leading to an increase in CMC_0 value with temperature [38]. This behaviour varies depending on the specific molecule under research. At high temperature, the Kc values generally decrease[39], however, Kinart in 2023 observed that in the case of HP-β-CDs and dodecanoic acid, the Kc values increased initially with temperature, reaching a maximum value at 25 °C, decreasing after that [38,40].

Hinze also described that the presence of salt in the reaction medium neutralizes the charge of micelles, thereby promoting their stability and formation. However, these changes may influence the system in different ways, depending on the specific compound involved and the characteristics of the surrounding medium [38]. Ionic strength plays a critical role not only in the initiation of micelle formation but also in the complexation behaviour with HP-β-CDs. The presence of salts markedly affects particle size. Particle size decreased substantially in PBS medium relative to MilliQ water. Specifically, for 50 μM Resv-4'-LA, the particle size observed in PBS medium was 600 nm, whereas in MilliQ water it was significantly reduced to 82 nm. Similarly, upon addition of 10 mM HP-β-CDs, the particle size decreased from 894 nm in PBS to 383 nm MilliQ water (Figure 6). Moreover, as shown in Table 2, the CMC_0 is higher in 100 mM PBS than in MilliQ water, indicating that the micelle formation began at lower LipoResv concentrations in MilliQ water.

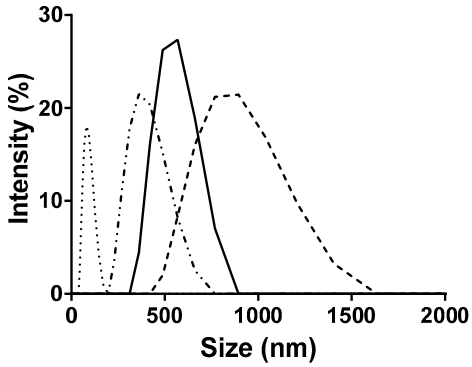

Figure 6. Particle size (nm) of Resv-4'-LA 50 μM (—), Resv-4'-LA 50 μM with 10 mM HP-β-CDs (- - -) in PBS and Resv-4'-LA 50 μM (˙˙˙˙) and Resv-4'-LA 50 μM with 10 mM HP-β-CDs (-··) in MilliQ water at 35 °C and pH 7.0.

The variation observed in the Kc as a function of different physio-chemical parameter values, underscore the high sensitivity of host–guest interactions within reaction media, as highlighted previously Hinze [38]. This intrinsic complexity offers the opportunity to finely modulate the encapsulation and release dynamics of active compounds such as LipoResv. Such tunability is particularly relevant for applications in controlled release systems, functional food formulation, and the design of molecular sensors.

Literature reports indicates that ionic strength can significantly influence both the micellization process and the resulting particle size. In PBS medium, higher concentration of LipoResv was required to initiate micellization. However, once micelles were formed the presence of ions in the medium promotes micellar aggregation, leading to an increase in particle size. In contrast, the absence of ions in MilliQ water, favours the formation of smaller micelles [41].

2.5. Computational Models

 doi:10.20944/preprints202507.0673.v1

The performed simulations hint that HP-β-CDs form stable inclusion complexes with a range of structurally diverse guests, including natural fatty acids (i.e., LA and DHA), their LipoResv (i.e., Resv-4′-LA and Resv-4′-DHA), and small model compounds such as resveratrol and diphenylhexatriene (DPHT). As illustrated in Figure 7, docking simulations showed consistent insertion of the hydrophobic portions of all guests into the CDs cavity. Even though that early docking results suggested a compatibility across all systems, a closer inspection of the inclusion poses reveals dissimilarities depending on the size and nature of the guest molecule.

Smaller compounds, such as resveratrol and DPHT, are fully accommodated within the internal cavity of HP-β-CDs. In contrast, the unmodified fatty acids LA and DHA exhibit partial insertion of their hydrophobic tails into the CDs cavity. Their relatively flexible carbon chains are located along with the apolar axis of the host, optimizing van der Waals contacts with the interior walls while leaving the carboxylic acid headgroup closer to the cavity entrance. These poses remain energetically favourable and are consistent with typical inclusion patterns reported for medium-chain fatty acids [42]. The most pronounced differences are observed for the LipoResv, Resv-4′-LA and Resv-4′-DHA. Due to their larger molecular size, these molecules exceed the spatial capacity of the CDs cavity. In their optimal docking poses, the resveratrol moiety is anchored within the CDs core, while the long hydrocarbon chains are located beyond the cavity opening and extends outward into the solvent. This arrangement reflects a compromise between maximizing favourable host–guest interactions and minimizing steric clashes and is further influenced by geometric constraints arising from the unsaturation in the fatty acid chains, especially in DHA, where kinks introduced by multiple double bonds reduce packing efficiency within the inner cavity.

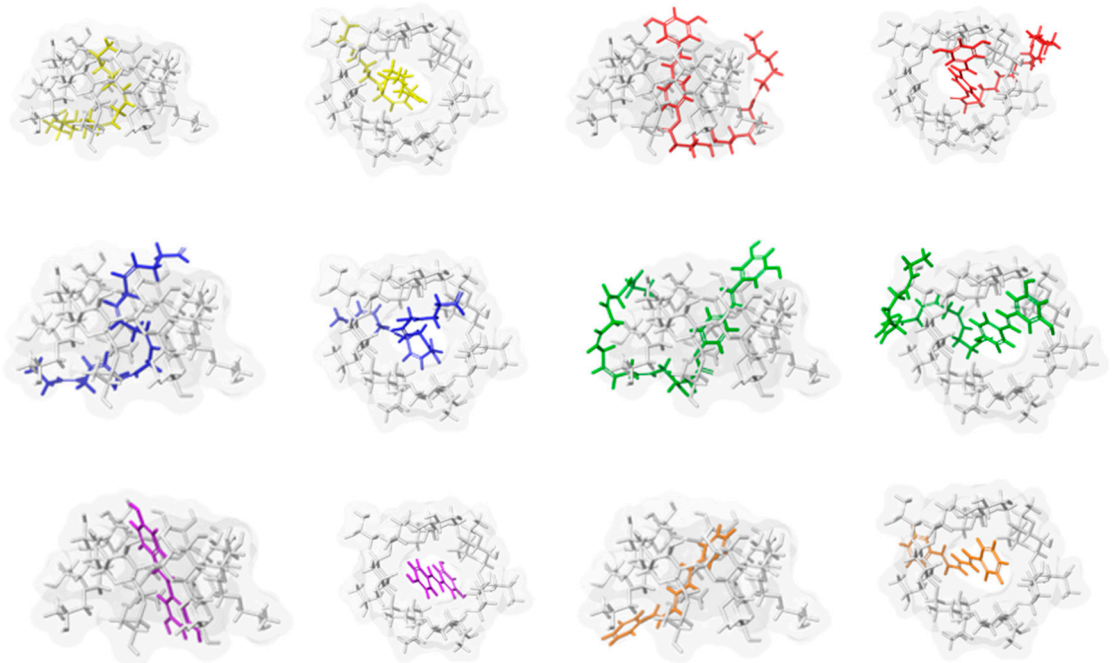

Figure 7. Docking poses corresponding to the most favourable host–guest interaction energies for HP-β-CDs inclusion complexes with six guest molecules: resveratrol (purple), diphenylhexatriene (DPHT) (orange), LA (yellow), DHA (blue), Resv-4′-LA (red), and Resv-4′-DHA (green). Cyclodextrins (CDs) are shown as stick-and-surface representations in grey, whereas guest molecules are rendered in coloured stick format. Two perspectives are shown for each complex: a front view and a lateral view, highlighting both internal accommodation and external extension of the guest structures.

Figure 6 captures these variations in encapsulation geometry, highlighting how the interplay between molecular size, flexibility, and hydrophobic–hydrophilic balance governs the inclusion mode. This qualitative analysis was further supported by binding free energy calculations. According

 doi:10.20944/preprints202507.0673.v1

to the MM-GBSA approach, HP-β-CDs exhibited a clear preference for larger and functionalized guests. The largest interaction energy (the most negative) was obtained for Resv-4′-LA (−64.36 kcal/mol), followed by Resv-4′-DHA (−58.34 kcal/mol), DHA (−51.05 kcal/mol), LA (−47.24 kcal/mol), DPHT (−47.38 kcal/mol), and finally resveratrol (−45.52 kcal/mol). These results suggested that LipoResv significantly enhances binding affinity, likely due to increased hydrophobic surface area and improved van der Waals complementarity within the HP-β-CDs cavity, in line with previous studies on amphiphilic guest molecules [43]. The numerical ranking also implies that both the native fatty acids and their LipoResv exhibited stronger binding than the fluorophore DPHT. These results confirm the departure of DPHT from the CDs cavity upon complexation with natural and modified fatty acids. Moreover, the original resveratrol showed the less intense interaction (less negative binding energy), highlighting how conjugation with LA or DHA improves complexation efficiency with HP-β-CDs.

However, our experimental data offer a contrasting picture. The experimentally determined Kc for LA was 7,432 M^{-1}, while that for Resv-4′-LA was only 719 M^{-1}, implying that LA forms a significantly more stable inclusion complex under identical conditions. This discrepancy suggested that absolute MM-GBSA binding energies alone may not provide a fully accurate representation of complex stability in solution, particularly when comparing ligands of different size and flexibility. To address this, we evaluated the ligand efficiency (LE), defined as the binding energy per heavy atom of the guest molecule. This normalized metric allows for a fairer comparison of guests with varying molecular size, which is our case [44,45].

Interestingly, LE values altered that ranking. LA showed the highest ligand efficiency (−2.362 kcal/mol per heavy atom), followed by DHA (−2.127 kcal/mol), Resv-4′-LA (−1.788 kcal/mol), and Resv-4′-DHA (−1.459 kcal/mol). These data suggested that although the LipoResv exhibit stronger absolute interactions, their per-atom binding efficiency is lower due to impact of entropic and packing effects. This trend aligns more closely with the experimental Kc values, where LA outperformed Resv-4′-LA by an order of magnitude. A similar trend is observed between Resv-4′-LA (Kc = 719 M^{-1}) and Resv-4′-DHA (Kc = 17 M^{-1}) (Table 1), confirming the superior performance of the Resv-4′-LA, both experimentally and computationally (in LE terms). The performed simulations hint the importance of implementing both absolute and normalized binding metrics in the theoretical assessment of inclusion complexes. While MM-GBSA highlights the cumulative interaction strength, LE offers a more balanced view for molecular packing efficiency in CDs related systems. This dual analysis strategy has been employed successfully in the design of host–guest systems and fragment-based drug discovery [44,46], and is particularly valuable here in explaining why smaller, more compact guests such as LA can outperform larger conjugates in real solution conditions (Table S2).

The computational protocol was finally completed by conducting MD simulations with a focus on assessing the micellization processes. As discussed above, the CMC value might be used as an indirect measure of surface activity and aqueous solubility. Under defined pH and temperature, this intrinsic property is denoted as CMC_0 and typically decreases with increasing hydrophobicity or chain length of the molecule [47]. Experimentally, Resv-4′-LA and Resv-4′-DHA, as well as their precursor fatty acids LA and DHA, showed increased relative fluorescence at concentrations above their respective CMC, confirming the formation of colloidal aggregates. As noted, experimental outcomes showed a striking difference between the two LipoResv: the CMC_0 of Resv-4′-LA was approximately 6,000 times higher than that of Resv-4′-DHA, indicating a much lower tendency of Resv-4′-LA to self-associate in aqueous medium. This discrepancy aligns with their physicochemical profiles—Resv-4′-DHA, bearing a longer and more unsaturated hydrophobic chain, exhibits greater surface activity and consequently a lower CMC_0, as expected from classical amphiphilic behaviour [48]. To complement these findings, atomistic MD simulations were carried out to model the formation and stabilization of micellar aggregates, as illustrated in Figure 8.

 doi:10.20944/preprints202507.0673.v1

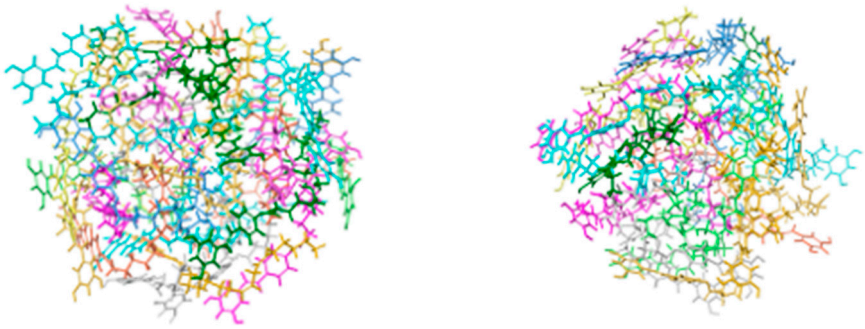

Figure 8. Designed models systems of micellar aggregates for Resv-4′-LA (left, contains 30 monomeric units) and Resv-4′-DHA (right, 24 units). The structures correspond to the clusters extracted from the final 100-ns simulation trajectories associated to the most favourable intermolecular interaction energies, as determined by MM-GBSA analysis. Micellar models are shown as coloured sticks.

The simulations confirmed the spontaneous micellar formation that allow for clustering to extract representative structures. The MM-GBSA interaction energy of a single unit within the micelle was next computed, providing a theoretical estimate of the cohesive strength within the aggregate

3. Materials and Methods

3.1. Materials

HP-β-CDs were provided by AraChem (Tilburg, Netherlands), LipoResv (Resv-4′-LA and Resv-4′-DHA) were obtained from Institute of Biomolecules Max Mousseron (IBMM), Pôle Chimie Balard Recherche, Montpellier (France). Free linoleic acid (LA), docosahexaenoic acid (DHA), diphenylhexatriene (DPHT) and tetrahydrofurane (THF) were purchased from Sigma Aldrich (Madrid, Spain). The rest of the chemical compounds used were of analytical grade.

3.2. Chemo-Enzymatic Synthesis of LipoResv

Resv-4′-La and Resv-4′-DHA were synthesized according to previous procedure [5,6] using enzymatic and chemical synthesis starting from resveratrol. The procedure was adapted for gram scale synthesis. In the first step, the supported lipase *Candida antartica* (CALB, Novozyme 435) was used to introduce acetyl group regio-selectively at the resveratrol C4⊛OH position. The reaction was performed in good yield (85%) without any acetyl derivatives in 3 or 5 positions. Hydroxyls at 3 and 5 positions were then protected by TIPS groups using TIPS-OTf and DIPEA as a base to obtain a 3,5-protected derivative. The acetyl group at the 4′position was deprotected with MeONa in anhydrous methanol and resulted resveratrol-3,5-diTIPS in excellent yield (90-95%). The coupling reactions between the silylated polyphenol and the selected fatty acid (LA or DHA) was initiated using DCC/DMAP as coupling reagent (74% for LA and 79 % for DHA). Final TIPS deprotection by Et_3N-3HF in dry tetrahydrofuran (THF) yielded Resv-4′-LA (88%) or Resv-4′-DHA (90%). ^{1}H-NMR analysis of the synthesized lipophenols were in accordance with literature.

3.3. Fluorimetric Determination of CMC

The CMC of fatty acids and LipoResv were determined by means the fluorescence spectroscopy method by Chattopadhyay, et al. in 1984 [49]. Increasing concentrations of different types of CDs were added to saturate buffered solutions of fatty acids or LipoResv at different pHs, using DPHT (in THF) as a fluorescent probe. The reaction medium contained in 2 mL of 100 mM sodium phosphate buffer (PBS) pH 7.0, MilliQ water (18 MΩ) pH 7.0, 100 mM sodium borate buffer pH 2.0 or pH 9.0; DPHT 0.89 μM (supplied in 20 μL of 10 % THF solution), 20 μL of fatty acid or LipoResv ethanolic solution and a given concentration of HP-β-CDs dissolved in the respective buffer or MilliQ water.

 doi:10.20944/preprints202507.0673.v1

The solutions were vortexed and given a N_2 flush prior to incubation in the dark for 60 minutes at different temperatures (35, 25 and 15 °C). Fluorescence intensity was measured at 430 nm (excitation wavelength 358 nm) using a SpectraMax iD3 plate reader equipped with a thermostat set at appropriate temperature, using a blank containing all reagents except LipoResv.

The CMC was determined graphically by plotting the relative fluorescence percentage *vs* fatty acid or LipoResv concentration, as the intersection between the post-micellar line fluorescence trend and the pre-micellar baseline.

3.4. Determination of Complexation Stoichiometry and Equilibrium Constant Between CDs and Fatty Acid or LipoResv

To characterise the formation of HP-β-CDs/LipoResv or HP-β-CDs/fatty acid inclusion complexes, the apparent CMC was plotted as a function of HP-β-CDs concentration, resulting in a micellar diagram indicating the inclusion complexes stoichiometry.

In the case of a post-micellar linear trend, a 1:1 stoichiometry is considered for inclusion complexes formation (20), and the complexation constant (Kc) was calculated by the following equation:

$$\mathrm{CMC} = CMC_0 + Kc * CMC_0[CDs] \quad (1)$$

where CMC_0 is the critical micellar concentration in the absence of CDs, which is characteristic for each compound at given pH, temperature and ionic strength. A linear representation of CMC *vs* [CDs] with a regression coefficient close to 1 indicates a 1:1 stoichiometry.

On the other hand, if the post-micellar trend fits a quadratic model, 1:2 stoichiometry is considered [14,17], where the complex is formed by sequential binding of 2 molecules of HP-β-CDs to 1 molecule of LipoResv or fatty acid, and the Kc are defined as follows:

$$K_1 = \frac{[LipoResv - CDs]}{[LipoResv][CDs]} \quad (2)$$

$$K_2 = \frac{[LipoResv - CD_2]}{[LipoResv - CDs][CDs]} \quad (3)$$

As highlighted by Bru et al. in 1995 [25], the fatty acid (or LipoResv in our case) concentration can be replaced by CMC in the presence of CDs and CMC_0 in their absence. Thus, the equilibrium constants K_1 and K_2 could be estimated using the following equation:

$$CMC = CMC_0 + K_1 CMC_0[CDs] + K_1 K_2 CMC_0[CDs]^2 \quad (4)$$

3.5. Determination of Particle Size by DLS

The size distribution and polydispersity index (PDI) of micelles was determined using a Zetasizer Red Ultra equipped with 10 mW red laser, at a scattering angle of 173° (backscatter) at 25 °C. Samples were prepared like in the case of fluorescent determination of CMC (see section 3.3), but without the fluorescent probe. To avoid interference from any particles present, all reagents were filtered through 0.22 µm nylon filter before sample preparation. After that, samples were prepared and incubated at 35 °C for 60 min to stabilize micelle formation. The samples were run in triplicate, and the resulting values represent the average of three runs, each comprising two measurements. Data analysis was performed using the integrated XZ XPLORER software to calculate particle size distribution.

To further assess the influence of ionic strength on micelle aggregation, CMC was investigated using two different media: MilliQ water and 100 mM PBS at pH 7.0.

3.6. Molecular Modelling

Computational models have been implemented to simulate the host–guest encapsulation processes. The initial three-dimensional structures of resveratrol, the fluorophore DPHT, and the

 doi:10.20944/preprints202507.0673.v1

unfunctionalized LA and DHA as well as their modified counterparts, Resv-4′-LA and Resv-4′-DHA, were generated using the Maestro software from Schrödinger, LLC [50]. The HP-β-CD host model was built using the same software and protocol. All molecular structures were prepared and optimized at neutral pH (7.0), consistent with experimental conditions, by using the LigPrep module from Schrödinger. This step included protonation state assignment, stereochemistry preservation, geometry minimization using the OPLS4 force field, and partial charge calculations [51].

Docking simulations were carried out using the Glide software (standard precision mode), allowing up to 10 poses per ligand to correctly explore conformational space [52]. The HP-β-CDs cavity was treated as a rigid host, while full ligand flexibility was enabled. Interaction energies obtained from docking were further refined through Molecular Mechanics/Generalized Born Surface Area (MM/GBSA) calculations using the Prime module [53]. These energies offer a more accurate approximation of binding affinities and are reported in Kcal/mol.

In addition to inclusion complexes, micellar models of functionalized fatty acids were built. These spherical assemblies mimic the amphiphilic nature of the Resv-4′-LA and Resv-4′-DHA conjugates, placing the polar resveratrol moieties toward the micelle surface and the hydrophobic alkyl chains toward the interior. For Resv-4′-LA, a total of 30 units were required to form a stable spherical configuration. In the case of Resv-4′-DHA, the higher degree of unsaturation reduces the number of compatible chains to 24, as larger numbers resulted in central overlap. Micelles were solvated in orthorhombic water boxes, with 10 Å buffer distance in all directions. Molecular dynamics (MD) simulations were then performed using the GPU-accelerated version of Desmond for 100 ns trajectories [54].

4. Conclusions

As highlighted by the results, the LipoResv compounds (Resv-4′-LA and Resv-4′-DHA) exhibit significantly greater hydrophobicity compared to their parent fatty acids. This enhanced hydrophobicity compared to their parent fatty acids. This enhanced hydrophobicity is reflected in their micellization behaviour, as evidenced by substantially lower CMC_0 values. These changes arise from the structural modification involving the conjugation of fatty acids to resveratrol, which alters their physicochemical properties. Moreover, this study demonstrates, for the first time, the potential of LipoResv compounds as self-assembling amphiphilic systems capable of forming stable inclusion complexes with HP-β-CDs. The host-guest interactions between LipoResv and HP-β-CDs were found to be highly dependent on the structural features of the guest molecules as well as the physicochemical conditions of the medium. Res-4′-LA is complexed by HP-β-CDs yielding 1:1 stoichiometry complex, whereas Res-4′-DHA form 1:2 complexes.

The performed computational simulations help us to complete the picture of the encapsulation and self-assembly equilibria associated to the novel LipoResv compounds. While absolute MMGBSA binding energies indicate stronger interactions for the LipoResv with HP-β-CDs, LE values reveal that smaller and more compact molecules, e.g., LA and DHA, lead to more efficiently on a per-atom basis, in agreement with complexation constants observed in the experiments. Furthermore, molecular dynamics simulations confirmed the ability of this complex ternary system to maintain the equilibrium between monomer LipoResv, self-assembling micelles and LipoResv-CDs complexes. Overall, the experimental results combined with multiscale modelling approaches underscore the relevance of this strategy in guiding the rational design of CDs-based encapsulation systems for poorly water-soluble bioactive phenolic compounds, as LipoResv, with potential applications in the pharmaceutical, nutraceutical and food science fields.

Supplementary Materials: The following supporting information can be downloaded at the website of this paper posted on Preprints.org, Table S1: Binding Affinities and Ligand Efficiencies for LipoResv with CDs. Best MMGBSA ΔG Bind (kcal/mol). Table S2: Best Ligand Efficiency (kcal/mol per heavy atom).

Author Contributions The authors who signed the following manuscript have made significant contributions, allowing them to achieve the set objectives. The synthesis and purification of the lipophenols used in this work

 doi:10.20944/preprints202507.0673.v1

was carried out by J.L., L.F., C.C. and T.D, also discussed the experiments, and wrote the manuscript. The size distribution and polydispersity index were accomplished by A.G.-I., also discussed the experiments and wrote the manuscript. A.B.H.-H. and D.A.S.-C. prepared, and performed the experiments, complexed lipophenols with cyclodextrins, gathered the data, analyzed the data, discussed the data, drew the figures, and wrote the manuscript. J.P.C.-C. carried out and interpreted the computational studies and also wrote the manuscript. E.N.-D. and J.A.G. were responsible for the conception, design and assessment of the work, gathered funding, supervised the writing of the manuscript, and wrote the final version of the manuscript. All authors have read and agreed to the published version of the manuscript.

Funding: This work was funded by the Spanish Ministry of Ministry of Science and Innovation (PID2020-120466RB-I00) and Fundación Séneca de la Región de Murcia (00009/COVI/20). The author A.B.H.-H. acknowledges a grant from Fundación Séneca de la Región de Murcia for the training of predoctoral research personnel.

Institutional Review Board Statement: Not applicable.

Informed Consent Statement: Not applicable.

Data Availability Statement: Not applicable.

Conflicts of Interest: The authors declare no conflict of interest.

References

1. Tomas-Barberan, F.A.; Andres-Lacueva, C. Polyphenols and health: current state and progress. J. Agric. Food Chem. 2012, 60(36), 8773-8775. https://doi.org/10.1021/acs.jafc.5b01173.
2. Shahidi, F.; Ambigaipalan, P. Omega-3 polyunsaturated fatty acids and their health benefits. *Annu. Rev. Food Sci. Technol.* **2018**, 9(1), 345-381. https://doi.org/10.1146/annurev-food-111317-095850.
3. Crauste, C.; Rosell, M.; Durand, T.; Vercauteren, J. Omega-3 polyunsaturated lipophenols, how and why? Biochimie. **2016**, 120, 62-74. https://doi.org/10.1016/j.biochi.2015.07.018.
4. Crauste, C.; Vercauteren, J.; Veas, F.; Durand, T.; Blondeau, N. Uses of lipophenolic compounds. U.S. Patent No. 11,419,841. 2022.Washington, DC: U.S. Patent and Trademark Office.
5. Moine, E.; Brabet, P.; Guillou, L.; Durand, T.; Vercauteren, J.; Crauste, C. New Lipophenol Antioxidants Reduce Oxidative Damage in Retina Pigment Epithelial Cells. *Antioxidants*. **2018**, *7* (12), 197. https://doi.org/10.3390/antiox7120197.
6. Shamseddin, A.; Crauste, C.; Durand, E.; Villeneuve, P.; Dubois, G.; Pavlickova, T.; Durand, T.; Vercauteren, J.; Veas, F. Resveratrol-Linoleate Protects from Exacerbated Endothelial Permeability via a Drastic Inhibition of the MMP-9 Activity. Biosci. Rep. **2018**, 38(4), BSR20171712. https://doi.org/10.1042/BSR20171712.
7. Silva, V.; Pórfido, J.L. Interacción de lípidos con el agua y formación de estructuras empaquetadas. In Análisis estructural y funcional de macromoléculas, 1st ed.; Córsico, B., Falomir-Lockhart, L.J., Franchini, G.R., Scaglia, N., Eds.; Universidad Nacional de La Plata, Buenos Aires, Argentina; 2013. pp. 193–219. https://doi.org/10.35537/10915/37269.
8. Göktürk, S.; Çalışkan, E.; Talman, R.Y.; Var, U. A study on solubilization of poorly soluble drugs by cyclodextrins and micelles: complexation and binding characteristics of sulfamethoxazole and trimethoprim. *Sci. World J.* **2012,** 1, 718791. https://doi.org/10.1100/2012/718791.
9. Von Krbek, L.K.S.; Schalley, C.A., Thordarson, P. Assessing cooperativity in supramolecular systems. *Chem. Soc. Rev.* **2017**, 46, 2622–2637. https://doi.org/10.1039/C7CS00063D.
10. Shalaby, K.S.; Ismail, M.I.; Lamprecht, A. Cyclodextrin Complex Formation with Water-Soluble Drugs: Conclusions from Isothermal Titration Calorimetry and Molecular Modeling. *AAPS Pharm. Sci. Tech.* **2021**, 22(7), 232. https://doi.org/10. 1208/s12249-021-02040-8.
11. Pérez-Abril, M.; Lucas-Abellán C.; Castillo-Sánchez, J.; Pérez-Sánchez, H.; Cerón Carrasco, J.P.; Fortea M. I.; Gabaldón J.A.; Núñez-Delicado E. Systematic investigation and molecular modelling of complexation between several groups of flavonoids and HP-β-cyclodextrins. *J. Funct. Foods*, **2017**, 36, 122-131. https://doi.org/10.1016/ j.jff.2017.06.052.

 doi:10.20944/preprints202507.0673.v1

12. Martín, V.I.; Ostos, F.J.; Angulo, M.; Márquez, A.M.; López-Cornejo, P.; López-López, M.; Carmona, A.T.; Moyá, M.L. Host-guest interactions between cyclodextrins and surfactants with functional groups at the end of the hydrophobic tail. *J. Colloid Interface Sci.* **2017**, 491, 336–48. https://doi.org/10.1016/j.jcis.2016.12.040.
13. Del Valle, E.M. Cyclodextrins and their uses: A review. *Process Biochem*. **2004**, 39(9), 1033–1046. https://doi.org/10.1016/S0032-9592(03)00258-9.
14. Saokham, P.; Muankaew, C.; Jansook, P.; Loftsson, T. Solubility of cyclodextrins and drug/cyclodextrin complexes. *Molecules*, **2018**, 23(5), 1161. https://doi.org/10.3390/molecules23051161.
15. Nicolaescu, O.E.; Ionescu, C.; Samide, A.; Tigae, C.; Spînu, C.I.; Oprea, B. Advancements in Cyclodextrin Complexes with Bioactive Secondary Metabolites and Their Pharmaceutical Applications. *Pharmaceutics*, **2025**, 17(4), 506. https://doi.org/10.3390/pharmaceutics17040506.
16. Rodríguez-López, M. I.; Mercader-Ros, M. T.; López-Miranda, S.; Pellicer, J. A.; Pérez-Garrido, A.; Pérez-Sánchez, H.; Núñez-Delicado, E.; Gabaldón, J. A. Thorough characterization and stability of HP-β-cyclodextrin thymol inclusion complexes prepared by microwave technology: A required approach to a successful application in food industry. *J. Sci. Food Agric.* **2019**, 99, 1322-1333. https://doi:10.1002/jsfa.9307.
17. Lucas-Abellán, C.; Gabaldón-Hernández, J.A.; Penalva, J.; Fortea, M.I.; Núñez-Delicado, E. Preparation and characterization of the inclusion complex of chlorpyrifos in cyclodextrins to improve insecticide formulations. *J. Agric. Food Chem*. **2008**, 56(17), 8081-8085. https://doi.org/10.1021/jf8015046.
18. Lucas-Abellán C.; Pérez-Abril, M.; Castillo, J.; Serrano, A.; Mercader-Ros, M.T.; Fortea, M.I.; Gabaldón, J.A.; Núñez-Delicado, E. Effect of temperature, pH, β- and HP-β-CDs on the solubility and stability of flavanones: Naringenin and hesperetin. *LWT-Food Sci. Technol*. **2019**, 108, 233-239. https://doi.org/10.1016/j.lwt.2019.03.059.
19. Moulik, S.P.; Rakshit, A.K.; Naskar, B. Evaluation of non-ambiguous critical micelle concentration of surfactants in relation to solution behaviors of pure and mixed surfactant systems: a physicochemical documentary and analysis. *J. Surfactants Deterg*. **2021**, 24(4), 535-549. https://doi.org/10.1002/jsde.12503.
20. Funasaki, N.; Ishikawa, S.; Neya, S. 1: 1 and 1: 2 complexes between long-chain surfactant and α-cyclodextrin studied by NMR. *J. Phys. Chem. B*. **2004**, 108(28), 9593-9598. https://doi.org/10.1021/jp0370268.
21. Scholz, N.; Behnke, T.; Resch-Genger, U. Determination of the critical micelle concentration of neutral and ionic surfactants with fluorometry, conductometry, and surface tension—a method comparison. *J. Fluoresc*. **2018**, 28, 465-476. https://doi.org/10.1007/s10895-018-2209-4.
22. Al-Soufi, W.; Piñeiro, L.; Novo, M. A model for monomer and micellar concentrations in surfactant solutions: Application to conductivity, NMR, diffusion, and surface tension data. *J. Colloid Interface Sci.* **2012**, 370(1), 102-110. https://doi.org/10.1016/j.jcis.2011.12.037.
23. Cabaleiro-Lago, C.; García-Río, L.; Hervés, P.; Mejuto, J.C.; Pérez-Juste, J. In search of fully uncomplexed cyclodextrin in the presence of micellar aggregates. *J. Phys. Chem. B*. **2006**, 110(32), 15831-15838. https://doi.org/10.1021/jp0626871.
24. Perinelli, D.R.; Cespi, M.; Lorusso, N.; Palmieri, G.F.; Bonacucina, G.; Blasi, P. Surfactant self-assembling and critical micelle concentration: one approach fits all? *Langmuir*, **2020**, 36(21), 5745-5753. https://doi.org/10.1021/acs.langmuir.0c00420.
25. Bru, R.; López-Nicolás, J.; García-Carmona, F. Aggregation of polyunsaturated fatty acids in the presence of cyclodextrins. *Colloid. Surf. A*. **1995**, 97(3), 263-269. https://doi.org/10.1016/0927-7757(95)03091-Q.
26. Matencio, A.; Hernández-Gil, C.J.G.; García-Carmona, F.; López-Nicolás, J.M. Physicochemical, thermal and computational study of the encapsulation of rumenic acid by natural and modified cyclodextrins. *Food Chem.* **2017**, 216, 289-295. https://doi.org/10.1016/j.foodchem.2016.08.023.
27. Degrand, L.; Garcia, R.; Urion, K.C.; Guiga, W. Dynamic light scattering for the determination of linoleic acid critical micelle concentration. Effect of pH, ionic strength, and ethanol. *J. Mol. Liq*. **2023**, 388, 122670. https://doi.org/10.1016/j.molliq.2023.122670.
28. Dorrego, B.; Garcia-Rio, L.; Hervés, P.; Leis, J.R.; Mejuto, J.C.; Pérez-Juste, J. Changes in the fraction of uncomplexed cyclodextrin in equilibrium with the micellar system as a result of balance between micellization and cyclodextrin−surfactant complexation. Cationic alkylammonium surfactants. *J. Phys. Chem. B*., **2001**, 105(21), 4912-4920. https://doi.org/10.1021/jp0035232.

 doi:10.20944/preprints202507.0673.v1

29. Matencio, A.; García-Carmona, F.; López-Nicolás, J.M. Aggregation of t10, c12 conjugated linoleic Acid in presence of natural and modified cyclodextrins. A physicochemical, thermal and computational analysis. *Chem. Phys. Lipids.* **2017**, 204, 57-64. https://doi.org/10.1016/j.chemphyslip.2017.03.008.
30. Connors, K. A. The stability of cyclodextrin complexes in solution. *Chem. Rev.* **1997**, 97(5), 1325-1358. https://doi.org/10.1021/cr960371r.
31. Triamchaisri, N.; Toochinda, P.; Lawtrakul, L. Structural Investigation of Beta-Cyclodextrin Complexes with Cannabidiol and Delta-9-Tetrahydrocannabinol in 1: 1 and 2: 1 Host-Guest Stoichiometry: Molecular Docking and Density Functional Calculations. *Int. J. Mol. Sci.* **2023**, 24(2), 1525. https://doi.org/10.3390/ijms24021525.
32. Dorrego, A.B.; García-Río, L.; Hervés, P.; Leis, J.R.; Mejuto, J.C.; Pérez-Juste, J. Micellization versus cyclodextrin–surfactant complexation. *Angew. Chem. Int. Ed.* **2000**, 39(16), 2945-2948. https://doi.org/10.1002/1521-3773(20000818)39:16<2945::AID-ANIE2945>3.0.CO;2-6.
33. Namani, T.; Ishikawa, T.; Morigaki, K.; Walde, P. Vesicles from docosahexaenoic acid. *Colloids Surf B Biointerfaces*. **2007**, 54(1), 118-123. https://doi.org/10.1016/j.colsurfb.2006.05.022.
34. Vinarov, Z.; Katev, V.; Radeva, D.; Tcholakova, S.; Denkov, N.D. Micellar solubilization of poorly water-soluble drugs: effect of surfactant and solubilizate molecular structure. *Drug Dev. Ind. Pharm.* **2018**, 44(4), 677-686. https://doi.org/10.1080/03639045.2017.1408642.
35. Ghosh, A.; Kanti Seth, S.; Purkayastha, P. Controlled formation of hydrated micelles by the intervention of cyclodextrins. *Chem. Plus. Chem.* **2019**, 84(1), 130-135. https://doi.org/10.1002/cplu.201800559.
36. Jiang, Y.B.; Wang, X.J. Direct evidence for β-cyclodextrin-induced aggregation of ionic surfactant below critical micelle concentration. *Appl. Spectrosc.* **1994**, 48(11), 1428-1431. https://opg.optica.org/as/abstract.cfm?URI=as-48-11-1428.
37. Tsianou, M.; Fajalia, A.I. Cyclodextrins and surfactants in aqueous solution above the critical micelle concentration: where are the cyclodextrins located?. *Langmuir*, **2014**, *30*(46), 13754-13764. https://doi.org/10.1021/la5013999.
38. Hinze, W.L. Fluorescence in Organized Assemblies. In *Encyclopedia of Analytical Chemistry: Applications, Theory and Instrumentation*, 1st ed.; Meyers R.A., Warner I.M., Eds. John Wiley & Sons, Ltd. Hoboken, New Jersey, USA, 2006. pp. 1–84. https://doi.org/10.1002/9780470027318.a5409.
39. Author 1, A.; Author 2, B. Title of the chapter. In *Book Title*, 2nd ed.; Editor 1, A., Editor 2, B., Eds.; Publisher: Publisher Location, Country, 2007; Volume 3, pp. 154–196.
40. Samuelsen, L.; Holm, R.; Schönbeck, C. Simultaneous determination of cyclodextrin stability constants as a function of pH and temperature–A tool for drug formulation and process design. *J. Drug Deliv. Sci. Tec.*, **2021**, 65, 102675. https://doi.org/10.1016/j.jddst.2021.102675.
41. Kinart, Z. Stability of the Inclusion Complexes of Dodecanoic Acid with α-Cyclodextrin, β-Cyclodextrin and 2-HP-β-Cyclodextrin. *Molecules*, **2023**, 28(7), 3113. https://doi.org/10.3390/molecules28073113.
42. Alopaeus, J.F.; Hagesæther, E.; Tho, I. Micellisation mechanism and behaviour of Soluplus®–furosemide micelles: Preformulation studies of an oral nanocarrier-based system. *Pharm.* **2019**, 12(1), 15. https://doi.org/10.3390/ph12010015.
43. Greenidge, P.A.; Kramer, C.; Mozziconacci, J.C.; Sherman, W. Improving docking results via reranking of ensembles of ligand poses in multiple X-ray protein conformations with MM-GBSA. *J. Chem. Inf. Model.* **2014**, 54(10), 2697-2717. https://doi.org/10.1021/ci5003735.
44. Hopkins, A.L.; Keserü, G.M.; Leeson, P.D.; Rees, D.C.; Reynolds, C.H. The role of ligand efficiency metrics in drug discovery. *Nat. Rev. Drug Discov.* **2014**, 13(2), 105-121. https://doi.org/10.1038/nrd4163.
45. Maffucci, I.; Contini, A. Explicit ligand hydration shells improve the correlation between MM-PB/GBSA binding energies and experimental activities. *J. Chem. Theory Comput.*, **2013**, 9(6), 2706-2717. https://doi.org/10.1021/ct400045d.
46. Suárez, D.; Díaz, N. Affinity Calculations of Cyclodextrin Host–Guest Complexes: Assessment of Strengths and Weaknesses of End-Point Free Energy Methods. *J. Chem. Inf. Model.* **2019**, 59(1), 421–440. https://doi.org/10.1021/acs.jcim.8b00805.
47. Maibaum, L.; Dinner, A.R.; Chandler, D. Micelle formation and the hydrophobic effect. *J. Phys. Chem. B.* **2004**, 108(21), 6778-6781. https://doi.org/10.1021/jp037487t.

 doi:10.20944/preprints202507.0673.v1

48. Rawicz, W.; Olbrich, K.C.; McIntosh, T.; Needham, D.; Evans, E. Effect of chain length and unsaturation on elasticity of lipid bilayers. *Biophys. J.* **2000**, 79(1), 328-339. https://doi.org/10.1016/S0006-3495.
49. Chattopadhyay, A.; London, E. Fluorimetric determination of critical micelle concentration avoiding interference from detergent charge. *Anal. Biochem*. **1984**, 139(2), 408-412. https://doi.org/10.1016/0003-2697(84)90026-5.
50. Schrödinger L. Schrödinger Release 2024 4: Maestro, LigPrep, Glide, Prime, Desmond. New York, NY: Schrödinger, LLC; 2024.
51. Roos, K.; Wu, C.; Damm, W.; Reboul, M.; Stevenson, J.M.; Lu, C.; Dahlgren, M.K.; Mondal, S.; Chen, W.; Wang, L.; Abel, R.; Friesner, R.A.; Harder, E.D. OPLS3e: Extending force field coverage for drug-like small molecules. *J. Chem. Theory Comput*. **2019**, 15(3), 1863-1874. https://doi.org/10.1021/acs.jctc.8b01026.
52. Friesner, R.A.; Banks, J.L.; Murphy, R.B.; Halgren, T.A.; Klicic, J.J.; Mainz, D.T.; Repasky, M.P.; Knoll, E.H.; Shelley, M.; Perry, J.K.; Shaw, D.E.; Francis, P.; Shenkin, P.S. Glide: a new approach for rapid, accurate docking and scoring. 1. Method and assessment of docking accuracy. *J. Med. Chem*. **2004**, 47(7), 1739-1749. https://doi.org/10.1021/jm0306430.
53. Lyne, P.D.; Lamb, M.L.; Saeh, J.C. Accurate prediction of the relative potencies of members of a series of kinase inhibitors using molecular docking and MM-GBSA scoring. *J. Med. Chem*. **2006**, 49(16), 4805-4808. https://doi.org/10.1021/jm060522a.
54. Bowers, K.J.; Chow, E.; Xu, H.; Dror, R.O.; Eastwood, M.P.; Gregersen, B.A.; Klepeis, J.L.; Kolossvary, I.; Moraes, M.A.; Sacerdoti, F.D.; Salmon, J.K.; Shan, Y.; Shaw, D.E. Scalable algorithms for molecular dynamics simulations on commodity clusters. In Proceedings of the 2006 ACM/IEEE Conference on Supercomputing (pp. 84-es). https://doi.org/10.1145/1188455.1188544.